Semantic Instance Segmentation via Deep Metric Learning

Alireza Fathi*   Zbigniew Wojna*   Vivek Rathod*   Peng Wang†   Hyun Oh Song*
Sergio Guadarrama*   Kevin P. Murphy*

Abstract

We propose a new method for semantic instance segmentation, by first computing how likely two pixels are to belong to the same object, and then by grouping similar pixels together. Our similarity metric is based on a deep, fully convolutional embedding model. Our grouping method is based on selecting all points that are sufficiently similar to a set of "seed points', chosen from a deep, fully convolutional scoring model. We show competitive results on the Pascal VOC instance segmentation benchmark.

1. Introduction

Semantic instance segmentation is the problem of identifying individual instances of objects and their categories (such as person and car) in an image. It differs from object detection in that the output is a mask representing the shape of each object, rather than just a bounding box. It differs from semantic segmentation in that our goal is not just to classify each pixel with a label (or as background), but also to distinguish individual instances of the same class. Thus, the label space is unbounded in size (e.g., we may have the labels "person-1", "person-2" and "car-1", assuming there are two people and one car). This problem has many practical applications in domains such as self-driving cars, robotics, photo editing, etc.

A common approach to this problem (e.g., [10, 4, 16, 6]) is first to use some mechanism to predict object bounding boxes (e.g., by running a class-level object detector, or by using a class agnostic box proposal method such as EdgeBoxes), and then to run segmentation and classification within each proposed box. However, this can fail if there is more than one instance inside of the box. Also, intuitively it feels more "natural" to first detect the mask representing each object, and then derive a bounding box from this, if needed. (Note that boxes are a good approximation to the shape of certain classes, such as cars and pedestrians, but they are a poor approximation for many other classes, such as articulated people, "wirey" objects like chairs, or

non-axis-aligned objects like ships seen from the air.)

Recently there has been a move towards "box-free" methods, that try to directly predict the mask for each object (e.g., [20, 21, 13, 17]). The most common approach to this is to modify the Faster RCNN architecture [23] so that at each point, it predicts a "centeredness" score (the probability the current pixel is the center of an object instance), a binary object mask, and a class label (rather than predicting the usual "objectness" score, bounding box, and class label). However, this approach requires that the entire object instance fits within the receptive field of the unit that is making the prediction. This can be difficult for elongated structures, that might span many pixels in the image. In addition, for some object categories, the notion of a "center" is not well defined.

In this paper, we take a different approach. Our key idea is that we can produce instance segmentations by computing the likelihood that two pixels belong to the same object instance and subsequently use these likelihoods to group similar pixels together. This is similar to most approaches to unsupervised image segmentation (e.g. [26, 8]), which group pixels together to form segments or "super-pixels". However, unlike the unsupervised case, we have a well-defined notion of what a "correct" segment is, namely the spatial extent of the entire object. This avoids ambiguities such as whether to treat parts of an object (e.g., the shirt and pants of a person) as separate segments, which plagues evaluation of unsupervised methods.

We propose to learn the similarity metric using a deep embedding model. This is similar to other approaches, such as FaceNet [25], which learn how likely two bounding boxes are to belong to the same instance (person), except we learn to predict the similarity of *pixels*, taking into account their local context.

Another difference from unsupervised image segmentation is that we do not use spectral or graph based partitioning methods, because computing the pairwise similarity of all the pixels is too expensive. Instead, we use compute the distance (in embedding space) to a set of K "seed points"; this can be implemented as tensor multiplication. To find these seed points, we learn a separate model that predicts how likely a pixel is to make a good seed; we call this the
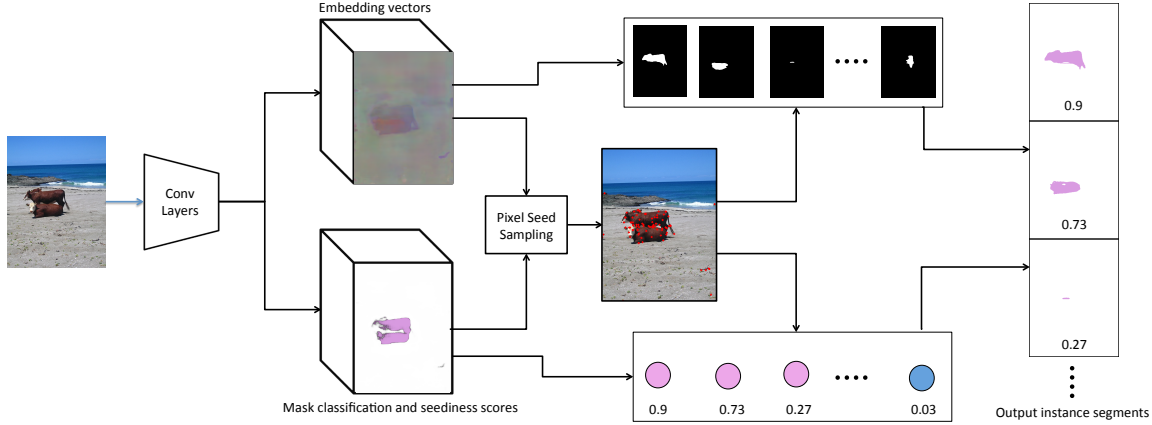
---

*Google Inc., USA
†UCLA

Figure 1. Given an image, our model predicts the embedding vector of each pixel (top head of the network) as well as the classification score of the mask each pixel will generate if picked as a seed (bottom head of the network). We derive the seediness scores from the classification scores and use them to choose which seed points in the image to sample. Each seed point generates a mask based on the embedding vectors; each mask is then associated with a class label and confidence score. In this figure, pink color corresponds to the "cow" class and blue to the "background" class.

"seediness" score of each pixel. This is analogous to the "centeredness" score used in prior methods, except we do not need to identify object centers; instead, the seediness score is a measure of the "typicality" of a pixel with respect to the other pixels in this instance. We show that in practice we only have to take the top 100 seeds to obtain good coverage of nearly all of the objects in an image.

Our method obtains a mAP score (at an IoU of 0.5) of 62.21 % on the Pascal VOC 2012 instance segmentation benchmark [7]. This puts us in fourth place, behind [16] (66.7%), [15] (65.7%), and [6] (63.5%). However, these are all proposal-based methods. (The previous fourth place method was the "proposal free" approach of [17], who obtained 58.7%.) Although not state of the art on this particular benchmark, our results are still competitive. Furthermore, we believe our approach may work particularly well on other datasets, with "spindly" objects with unusual shapes, although we leave this to future work.

2. Related work

The most common approach to instance segmentation is first to predict object bounding boxes, and then to predict the mask inside of each such box using one or more steps. For example, the MNC method of [6], which won the COCO 2015 instance segmentation competition, was based on this approach. In particular, they modified the Faster RCNN method [23] as follows: after detecting the top K boxes, and predicting their class labels, they extract features for each box using ROI pooling applied to the feature map and use this to predict a binary mask representing the shape of the corresponding object instance. The locations of the boxes can be refined, based on the predicted mask, and the process repeated. [6] iterated this process twice, and the R2-
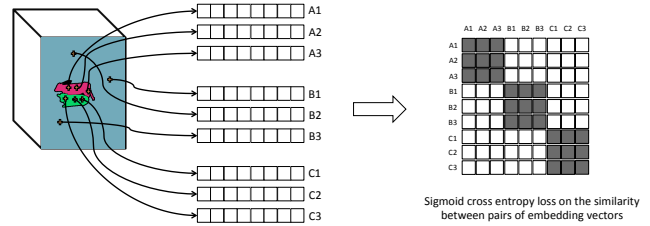

Figure 2. We compute the embedding loss by sampling the embedding vector of K pixels within each instance, resulting in a total of NK embedding vectors where N is the number of instances in image. We compute the similarity between every pair of embedding vectors $\sigma(e_p, e_q)$ as described in Eq. 1. We want to learn a metric that returns a similarity of 1 for a pair of embedding vectors that belong to the same instance, and 0 for a pair of embedding vectors that belong to different instances. Thus, we add a cross entropy loss on the similarity between pairs by setting the ground-truth values to 0 and 1 based on whether embedding vectors belong to the same instance or not.

IOS method in [16] iterated the process a variable number of times.

The fully convolutional instance segmentation method of [15] won the COCO instance segmentation challenge in 2016. It leverages the position sensitive score maps used in the mask proposal mechanism of [5]. At each location, it predicts a mask, as well as a category likelihood. DeepMask [20] and SharpMask [21] use a similar approach, without the position-sensitive score maps. Note that most of these sliding window methods used an image pyramid to handle objects of multiple sizes. Recently, [18, 13] proposed to use a feature pyramid network instead of recomputing features on an image pyramid.

The above methods all operate in parallel across the

whole image. Alternatively, we can run sequentially, extracting one object instance at a time. [24] and [22] are examples of this approach. In particular, they extract features using a CNN and then use an RNN to "emit" a binary mask (corresponding to an object instance) at each step. The hidden state of the RNN is image-shaped and keeps track of which locations in the image have already been segmented. The main drawback of this approach is that it is slow. Also, it is troublesome to scale to large images, since the hidden state sequence can consume a lot of memory.

An another way to derive a variable number of objects (regions) is to use the watershed algorithm. The method of [2] predicts a (discretized) energy value for each pixel. This energy surface is then partitioned into object instances using the watershed algorithm. The process is repeated independently for each class. The input to the network is a 2d vector per pixel, representing the direction away from the pixel's nearest boundary; these vectors are predicted given an RGB input image. The overall approach shows state of the art results on the CityScapes dataset. (A similar approach was used in [28], except they used template matching to find the instances, rather than watershed; also, they relied on depth data during training.)

Kirrilov et al. [14] also use the watershed algorithm to find candidate regions, but they apply it to an instance-aware edge boundary map rather than an energy function. They extract about 3000 instances (superpixels), which become candidate objects. They then group (and apply semantic labels) to each such region by solving a Multi-Cut integer linear programming optimization problem.

Although the watershed algorithm has some appeal, these techniques cannot group disconnected regions into a single instance (e.g., if the object is partitioned into two pieces by an occluder, such as the horse in Figure6 who is occluded by its rider). Therefore, we consider more general clustering algorithms. Newel and Deng [19] predict an objectness score for each pixel, as well as a one-dimensional embedding for each pixel. They first threshold on the objectness heatmap to produce a binary mask. They then compute a 1d histogram of the embeddings of all the pixels inside the mask, perform NMS to find modes, and then assign each pixel in the mask to its closest centroid.

Our approach is related to [19], but differs in the following important ways: (1) we use a different loss function when learning the pixel similarity metric; (2) we use a different way of creating masks, based on identifying the basins of attraction in similarity space, rather than using a greedy clustering method; (3) we learn a D-dimensional embedding per pixel, instead of using 1d embeddings. As a consequence, our results are much better: we get a mAP^r (at an IoU of 0.5) of 62.21 % on PASCAL VOC 2012 validation, whereas [19] gets 35.1%.

3. Method

In the following sections, we describe our method in more detail.

3.1. Overview of our approach

We start by taking a model that was pretrained for semantic segmentation (see Section 3.5 for details), and then modify it to perform instance segmentation by adding two different kinds of output "heads". The first output head produces embedding vectors for each pixel. Ideally, embedding vectors which are similar are more likely to belong to the same object instance. In the second head, the model predicts a class label for the mask centered at each pixel, as well as a confidence score that this pixel would make a good "seed" for creating a mask. We sketch the overall model in Figure 1, and give the details below.

3.2. Embedding model

We start by learning an embedding space, so that pixels that correspond to the same object instance are close, and pixels that correspond to different objects (including the background) are far. The embedding head of our network takes as input a feature map from a convolutional feature extractor (see Section 3.5). It outputs a $[h, w, d]$ tensor (as shown in Figure 1), where h is the image height, w is the image width and d is the embedding space dimension (we use 64 dimensional embeddings in our experiments). Thus each pixel p in image is represented by a d-dimensional embedding vector e_p.

Given the embedding vectors, we can compute the similarity between pixels p and q as follows:

$$\sigma(p, q) = \frac{2}{1 + \exp(||e_p - e_q||_2^2)} \qquad (1)$$

We see that for pairs of pixels that are close in embedding space, we have $\sigma(p, q) = \frac{2}{1+e^0} = 1$, and for pairs of pixels that are far in embedding space, we have $\sigma(p, q) = \frac{2}{1+e^\infty} = 0$.

We train the network by minimizing the following loss:

$$\mathcal{L}_e = -\frac{1}{|S|} \sum_{p,q \in S} w_{pq} \left[1_{\{y_p = y_q\}} \log(\sigma(p, q)) \right.$$
$$\left. + 1_{\{y_p \neq y_q\}} \log(1 - \sigma(p, q)) \right]$$

where S is the set of pixels that we choose, y_p is the instance label of pixel p, and w_{pq} is the weight of the loss on the similarity between p and q. The weights w_{pq} are set to values inversely proportional to the size of the instances p and q belong to, so the loss will not become biased towards the larger examples. We normalize weights so that $\sum_{p,q} w_{pq} = 1$.
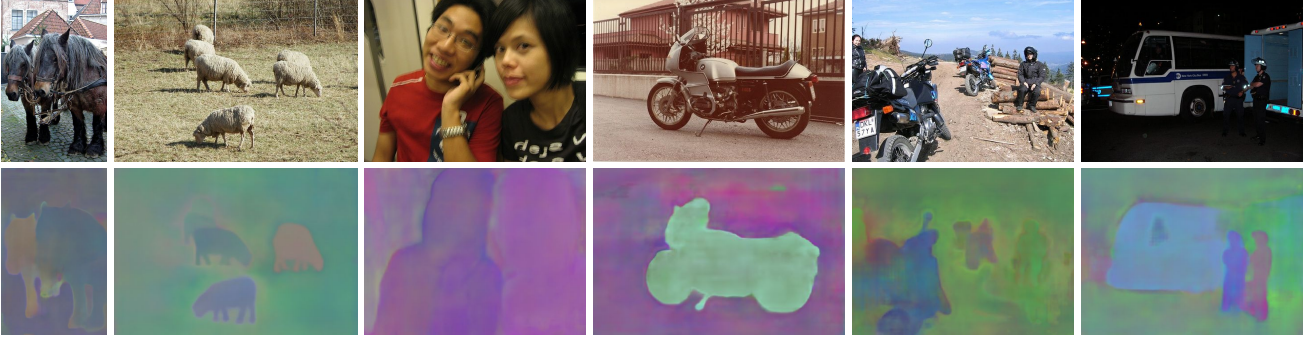
Figure 3. Visualization of the embedding vectors by randomly projecting the 64 dimensional vectors into RGB space. The learned metric will move different instances of the same object category to different locations in embedding space.

During training, we choose the set of pixels S by randomly sampling K points for each object instance in the image. For each pair of points, we compute the target label, which is 1 if they are from the same instance, and 0 otherwise, as shown in Figure 2. We then minimize the cross-entropy loss for the $|S|^2$ set of points. Our overall procedure is closely related to the N-pairs loss used in [27] for metric learning.

Figure 3 illustrates the learned embedding for few example images. We randomly project the 64d vectors to RGB space and then visualize the resulting false-color image. We see that instances of the same class (e.g., the two people or the two motorbikes) get mapped to different parts of embedding space, as desired.

3.3. Creating masks

Once we have an embedding space, and hence a pairwise similarity metric, we create a set of masks in the following way. We pick a "seed" pixel p, and then "grow" the seed by finding all the other pixels q that have a similarity with p greater than a threshold τ: $m(p, \tau) = \{q : \sigma(p, q) \geq \tau\}$. Ideally, all the pixels in the mask belong to the same object as the seed p. By varying τ, we can detect objects of different sizes. In our experiments, we use $\tau \in \{0.25, 0.5, 0.75\}$. (We also use a multi-scale representation of the image as input, as we discuss in Section 3.6.)

We can implement this method efficiently as follows. First we compute a tensor A of size $[h, w, d]$ (where h is the height of the image, w is the width, and d is the emebdding dimension) representing the embedding vector for every pixel. Next we compute a second tensor B of size $[k, d]$, representing the embedding vector of the K seed points. We can compute the distance of each vector in A to each vector in B using $A^2 + B^2 - 2A \odot B$. We can then select all the pixels that are sufficiently similar to each of the seeds by thresholding this distance matrix.

Fig. 4 shows examples of mask growing from randomly picked seed pixel. The seed pixel is noted by a red mark in the image. The similarity between every pixel and the
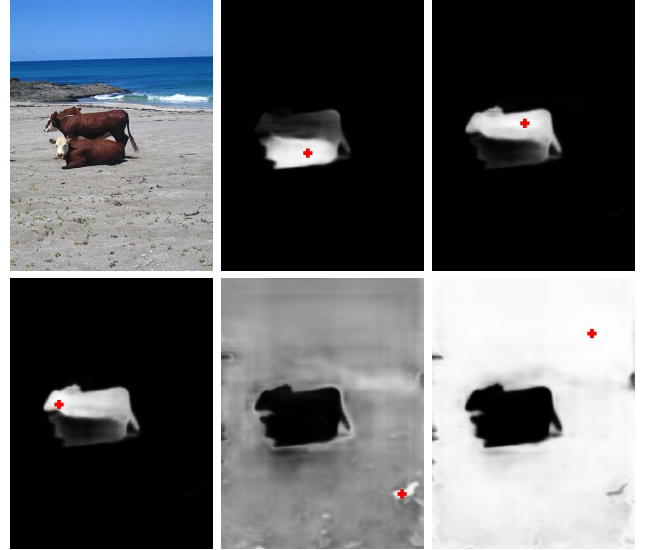

Figure 4. We visualize the similarity of each pixel and a randomly chosen seed pixel in each image. The randomly chosen seed pixel is shown by a red mark in the image. The brighter the pixels the higher the similarity.

seed pixel is computed based on Eq. 1 and shown in each picture. One can threshold the similarity values to generate a binary mask.

However, we still need a mechanism to choose the seeds. We propose to learn a "seediness" heatmap S_p, which tells us how likely it is that a mask grown from p will be a good mask (one that overlaps with some ground truth mask by more than an IoU threshold). We discuss how to compute the seediness scores in Section 3.4.

Once we have the seediness heatmap, we can greedily pick seed points based on its modes (peaks). However, we also want to encourage spatial diversity in the locations of our seed points, so that we ensure our proposals have high coverage of the right set of masks. For this reason, we also compute the distance (in embedding space) between each point and all previously selected points and choose one that

Figure 5. Visualization of sampled seed pixels. Our method leverages the learned distance metric and masks classification scores to sample high-quality seed pixels that result in instance segments that have high recall and precision.

is far from the already picked points (similar to the heuristic used by Kmeans++ initialization [1]). More precisely, at step t of our algorithm, we select a seed point as follows:

$$p_t = \arg \max_{p \notin p_{1:t-1}} \left[\log(S_p) + \alpha \log(D(p, p_{1:t-1})] \right.$$

where

$$D(p, p_{1:t-1}) = \min_{q \in p_{1:t-1}} ||e_p - e_q||_2^2$$

Selecting seed pixels with high seediness score guarantees high precision, and selecting diverse seed points guarantees high recall. Note that our sampling strategy is different from the non-maximum suppression algorithm. In NMS, points that are close in x-y image coordinate space are suppressed, while in our algorithm, we encourage diversity in the embedding space.

Once we have selected a seed, we select the best threshold τ, and then we can convert it into a mask, $m_t = m(p_t, \tau)$, as we described above. Finally, we attach a confidence score s_t and a class label c_t to the mask. To do this, we leverage a semantic-segmentation model which associates a predicted class label with every pixel, as we explain in Section 3.4.

3.4. Classification and seediness model

The mask classification head of our network takes as input a feature map from a convolutional feature extractor (see Section 3.5) and outputs a $[h, w, C + 1]$ tensor as shown in Fig. 1, where C is the number of classes, and label 0 represents the background. In contrast to semantic segmentation, where the pixels themselves are classified, here we classify the mask that each pixel will generate if chosen as a seed. For example, assume a pixel falls inside an instance of a horse. Semantic segmentation will produce a high score for class "horse" at that pixel. However, our method might instead predict background, if the given pixel is not a good seed point for generating a horse mask. We show examples of mask classification heatmaps in Fig. 6. We see that most pixels inside the object make good seeds, but pixels near the boundaries (e.g., on the legs of the cows) are not so good.

We train the model to emulate this behavior as follows. For each image, we select $K = 10$ random points per object instance and grow a mask around each one. Let $m(p, \tau)$ be the mask generated from pixel p, for a given similarity

threshold τ. If the proposed mask overlaps with one of the ground truth masks by more than some fixed IoU threshold, we consider this a "good" proposal; we then copy the label from the ground truth mask and assign it to pixel p. If the generated mask does not sufficiently overlap with any of the ground truth masks, we consider this a "bad" proposal and assign the background label to pixel p. We then convert the assigned labels to one-hot form, and train using softmax cross-entropy loss, for each of the K chosen points per object instance. The classification model is fully convolutional, but we only evaluate the loss at NK points, where N is the number of instances. Thus our overall loss function has the form

$$\mathcal{L}_{cls} = -\frac{1}{|S|} \sum_{p \in S} \sum_{c=0}^{C} y_{pc} \log \mathcal{C}_{pc}$$

where $\mathcal{C}_{pc}$ is the probability that the mask generated from seed pixel p belongs to class c.

To handle objects of different sizes, we train a different classification model for each value of τ; in our experiments, we use $\mathcal{T} = \{0.25, 0.5, 0.75, 0.9\}$. Specifically, let $\mathcal{C}_{pc}^{\tau}$ represent the probability that pixel p is a good seed for an instance class c when using similarity threshold τ.

We now define the "seediness" of pixel p to be

$$S_p = \max_{\tau \in \mathcal{T}} \max_{c=1}^{C} \mathcal{C}_{pc}^{\tau}$$

(Note that the max is computed over the object classes and not on the background class.) Thus we see that the seediness tensor is computed from the classification tensor.

To understand why this is reasonable, suppose the background score at pixel p is very high, say 0.95. Then the max over foreground classes is going to be smaller than 0.05 (due to the sum-to-one constraint on $\mathcal{C}_{pc}$), which means this is not a valid pixel to generate a mask. But if the max value is, say, 0.6, this means this is a good seed pixel, since it will grow into an instance of foreground class with probability 0.6.

Once we have chosen the best seed according to S_p, we can find the corresponding best threshold τ, and label c by computing

$$(\tau_p, c_p) = \arg \max_{\tau \in \mathcal{T}, c \in 1:C} \mathcal{C}_{pc}^{\tau}$$

Figure 6. Visualization of mask classification scores. The color at each pixel identifies the label of the mask that will be chosen if that pixel is chosen as a seed point. The pixels that are more likely to generate background masks are colored white. Darker colors correspond to pixels that will generate poor quality foreground masks. Brighter colors correspond to pixels that generate high quality masks.

The corresponding confidence score is given by

$$s_p = \mathcal{C}_{p,c_p}^{\tau_p}$$

3.5. Shared full image convolutional features

Our base feature extractor is based on the DeepLab v2 model [3], which in turn is based on resnet-101 [11]. We pre-train this for semantic segmentation on COCO, as is standard practice for methods that compete on PASCAL VOC, and then "chop off" the final layer. The Deeplab v2 model is fully convolutional and runs on an image of size $[2h, 2w, 3]$ outputs a $[\frac{h}{4}, \frac{w}{4}, 2048]$ sized feature map which is the input to both the embedding model and the classification/seediness model.

We can jointly train both output "heads", and backprop into the shared "body", by defining the loss

$$\mathcal{L} = \mathcal{L}_e + \lambda \mathcal{L}_{cls}$$

where $\mathcal{L}_e$ is the embedding loss, $\mathcal{L}_{cls}$ is the classification loss, and λ is a balancing coefficient. In our experiments, we initially set λ to 0, to give the embedding model time to learn proper embeddings. Once we have a reasonable similarity metric, we can start to learn the mask classification loss. We gradually increase λ to a maximum value of 0.2 (this was chosen empirically based on the validation set). Both losses get back-propagated into the same feature extractor. However, since we train on Pascal VOC, which is a small dataset, we set the learning rate of the shared features to be smaller than for the two output heads, so the original features (learned on COCO) do not change much.

3.6. Handling scale

To handle objects of multiple scales, we compute an image pyramid at 4 scales (0.25, 0.5, 1.0, 2.0), and then run it through our feature extractor These feature maps are then rescaled to the same size, and averaged. Finally, the result is fed into the two different heads, as explained above. (In the future, we would like to investigate more efficient methods, such as those discussed in [13, 18]. that avoid having to run the base model 4 times.)

4. Results

In this section, we discuss our experimental results.

4.1. Experimental Setup

We follow the experimental protocol that is used by previous state of the art methods [16, 15, 17, 4, 10]. In particular, we train on the PASCAL VOC 2012 training set, with additional instance mask annotation from [9], and we evaluate on the PASCAL VOC 2012 validation set.

After training the model, we compute a precision-recall curve for each class, based on all the test data. This requires a definition of what we mean by a true and false positive. We follow standard practice and say that a predicted mask that has an intersection over union IoU with a true mask above some threshold β (e.g. 50%) is a true positive, unless the true mask is already detected, in which case the detection is a false positive. We provide results for three IoU thresholds: $\{0.5, 0.6, 0.7\}$ similar to previous work. We then compute the area under the PR curve, known as the "average precision" or AP^r score [9]. Finally, we average this over classes, to get the mean average precision or mAP^r score.

We can also evaluate the quality of our method as a "class agnostic" region proposal generator. There are two main ways to measure quality in this case. The first is to plot the recall (at a fixed IoU) vs the number of proposals. The second is to plot the recall vs the IoU threshold for a fixed number of proposals; the area under this curve is known as the "average recall" or AR [12].

4.2. Preprocessing

We use the following data augmentation components during training:

Random Rotation: We rotate the training images by a random degree in the range of $[-10, 10]$.

Random Resize: We resize the input image during the training phase with a random ratio in the range of $[0.7, 1.5]$.

Random Crop: We randomly crop the images during the training phase. At each step, we randomly crop 100 windows. We randomly sample one image weighted towards
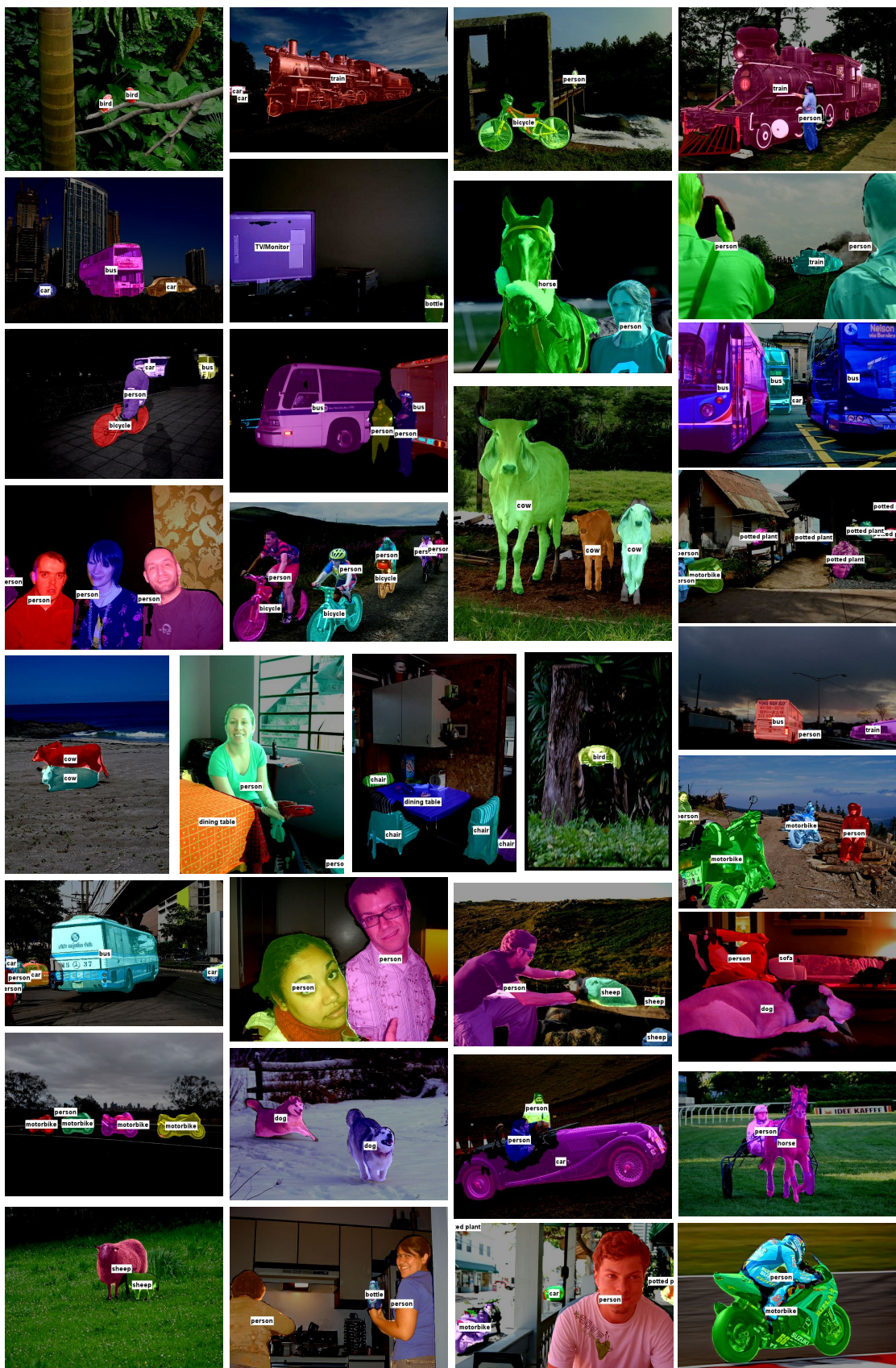
Figure 7. Example instance segmentation results from our method.

Table 1. Per-class instance-level segmentation comparison using APr metric over 20 classes at 0.5, 0.6 and 0.7 IoU on the PASCAL VOC 2012 validation set. All numbers are in %.

IoU score	Method	plane	bike	bird	boat	bottle	bus	car	cat	chair	cow	table	dog	horse	motor	person	plant	sheep	sofa	train	tv	average
0.5	SDS [10]	58.8	0.5	60.1	34.4	29.5	60.6	40.0	73.6	6.5	52.4	31.7	62.0	49.1	45.6	47.9	22.6	43.5	26.9	66.2	66.1	43.8
	Chen et al. [4]	63.6	0.3	61.5	43.9	33.8	67.3	46.9	74.4	8.6	52.3	31.3	63.5	48.8	47.9	48.3	26.3	40.1	33.5	66.7	67.8	46.3
	PFN [17]	76.4	15.6	74.2	54.1	26.3	73.8	31.4	92.1	17.4	73.7	48.1	82.2	81.7	72.0	48.4	23.7	57.7	64.4	88.9	72.3	58.7
	MNC [6]	-	-	-	-	-	-	-	-	-	-	-	-	-	-	-	-	-	-	-	-	63.5
	Li et al. [15]	-	-	-	-	-	-	-	-	-	-	-	-	-	-	-	-	-	-	-	-	65.7
	R2-IOS [16]	87.0	6.1	90.3	67.9	48.4	86.2	68.3	90.3	24.5	84.2	29.6	91.0	71.2	79.9	60.4	42.4	67.4	61.7	94.3	82.1	66.7
	Assoc. Embedding [19]	-	-	-	-	-	-	-	-	-	-	-	-	-	-	-	-	-	-	-	-	35.1
	Ours	69.7	1.2	78.2	53.8	42.2	80.1	57.4	88.8	16.0	73.2	57.9	88.4	78.9	80.0	68.0	28.0	61.5	61.3	87.5	70.4	62.1
0.6	SDS [10]	43.6	0	52.8	19.5	25.7	53.2	33.1	58.1	3.7	43.8	29.8	43.5	30.7	29.3	31.8	17.5	31.4	21.2	57.7	62.7	34.5
	Chen et al. [4]	57.1	0.1	52.7	24.9	27.8	62.0	36.0	66.8	6.4	45.5	23.3	55.3	33.8	35.8	35.6	20.1	35.2	28.3	59.0	57.6	38.2
	PFN [17]	73.2	11.0	70.9	41.3	22.2	66.7	26.0	83.4	10.7	65.0	42.4	78.0	69.2	72.0	38.0	19.0	46.0	51.8	77.9	61.4	51.3
	R2-IOS [16]	79.7	1.5	85.5	53.3	45.6	81.1	62.4	83.1	12.1	75.7	20.2	81.5	49.7	63.9	51.2	35.7	56.2	56.7	87.9	78.8	58.1
	Ours	64.2	0.1	64.8	37.2	34.5	73.5	50.6	83.4	8.9	59.4	48.2	84.3	65.1	69.6	56.6	14.9	51.8	50.7	81.7	64.4	53.3
0.7	SDS [10]	17.8	0	32.5	7.2	19.2	47.7	22.8	42.3	1.7	18.9	16.9	20.6	14.4	12.0	15.7	5.0	23.7	15.2	40.5	51.4	21.3
	Chen et al. [4]	40.8	0.07	40.1	16.2	19.6	56.2	26.5	46.1	2.6	25.2	16.4	36.0	22.1	20.0	22.6	7.7	27.5	19.5	47.7	46.7	27.0
	PFN [17]	68.5	5.6	60.4	34.8	14.9	61.4	19.2	78.6	4.2	51.1	28.2	69.6	60.7	60.5	26.5	9.8	35.1	43.9	71.2	45.6	42.5
	MNC [6]	-	-	-	-	-	-	-	-	-	-	-	-	-	-	-	-	-	-	-	-	41.5
	Li et al. [15]	-	-	-	-	-	-	-	-	-	-	-	-	-	-	-	-	-	-	-	-	52.1
	R2-IOS [16]	54.5	0.3	73.2	34.3	38.4	71.1	54.0	76.9	6.0	63.3	13.1	67.0	26.9	39.2	33.2	25.4	44.8	45.4	81.5	74.6	46.2
	Assoc. Embedding [19]	-	-	-	-	-	-	-	-	-	-	-	-	-	-	-	-	-	-	-	-	26.0
	Ours	53.0	0.0	51.8	24.9	21.9	69.2	40.1	76.6	4.1	43.1	21.1	74.4	44.7	54.3	40.3	7.5	40.5	39.6	69.5	52.6	41.5

α	0.1	0.2	0.3	0.4	0.5	0.6
mAP^r	61.4	61.7	**62.1**	61.6	61.6	61.5

Table 2. We find out that the best performing α parameter for sampling seed points is 0.3. In the table, we compare the mAPr performance for different values of α.

Number of samples	10	20	30	40	50	60	70	80	90	100	200	500	1000
AR at 50% IOU	55.8	58.5	61.0	63.0	65.2	66.7	68.4	69.8	70.8	71.9	77.4	82.2	83.6
mAP^r with $\alpha = 0.2$	59.7	60.7	60.7	60.9	61.2	61.3	61.1	61.1	61.0	61.0	61.4	61.5	61.7

Table 3. We analyze the performance of our model given the number of sampled seed points.

cropped windows that have more object instances inside.

Random Flip: We randomly flip our training images horizontally.

4.3. Results on Pascal VOC 2012

We first tried different values of α (which trades off diversity with seediness when picking the next seed) to find the best performing seed sampling strategy. The results are shown for different values of α in Table 2. We also tried various sizes of embeddings from 2 to 256; 64 was best (on a validations set). We furthermore analyze the performance of our model given different number of mask proposals (number of sampled seed points) in Table 3. Our model reaches a mAP^r performance of 59.7 by only proposing 10 regions. In Table 3, we also show the class agnostic average recall for different number of mask proposals.

Figure 7 shows some qualitative results, and Table 1 shows our quantitative results. In terms of mAP performance, we rank 4th at 0.5 IoU threshold, 2nd at 0.6 IoU threshold, and tied 3rd at 0.7 IoU threshold. So our method

is competitive, if not state of the art.

Regarding performance for individual classes, we see that we do very well on large objects, such as trains, dogs, and motorbikes, but we do very poorly in the bicycle category. (See Fig. 6 for some examples.) This is also true of the other methods. The reason is that there is a large discrepancy between the quality of the segmentation masks in the training set of [9] compared to the PASCAL test set. In particular, the training set uses a coarse mask covering the entire bicycle, whereas the test set segments out each spoke of the wheels individually.

5. Conclusion and future work

We have proposed a novel approach to the semantic instance segmentation problem, and obtained promising preliminary results on the PASCAL VOC dataset. In the future, we would like to evaluate our method on COCO and Cityscapes. We would also like to devise a way to perform region growing in a differentiable way so that we can perform end-to-end training.

References

[1] D. Arthur and S. Vassilvitskii. k-means++: The advantages of careful seeding. *Proc. symposium on discrete algorithms*, 2007. 5

[2] M. Bai and R. Urtasun. Deep watershed transform for instance segmentation. 24 Nov. 2016. 3

[3] L.-C. Chen, G. Papandreou, I. Kokkinos, K. Murphy, and A. L. Yuille. DeepLab: Semantic image segmentation with deep convolutional nets, atrous convolution, and fully connected CRFs. *IEEE PAMI*, 2017. 6

[4] Y.-T. Chen, X. Liu, and M.-H. Yang. Multi-instance object segmentation with occlusion handling. In *Proceedings of the IEEE Conference on Computer Vision and Pattern Recognition*, pages 3470–3478, 2015. 1, 6, 8

[5] J. Dai, K. He, Y. Li, S. Ren, and J. Sun. Instance-sensitive fully convolutional networks. In *ECCV*, 2016. 2

[6] J. Dai, K. He, and J. Sun. Instance-aware semantic segmentation via multi-task network cascades. In *CVPR*, 2016. 1, 2, 8

[7] M. Everingham, S. M. Ali Eslami, L. Van Gool, C. K. I. Williams, J. Winn, and A. Zisserman. The pascal visual object classes challenge: A retrospective. *Intl. J. Computer Vision*, 111(1):98–136, 25 June 2014. 2

[8] P. F. Felzenszwalb and D. P. Huttenlocher. Efficient Graph-Based image segmentation. *Intl. J. Computer Vision*, 59(2):167–181, 1 Sept. 2004. 1

[9] B. Hariharan, P. Arbelaez, L. Bourdev, S. Maji, and J. Malik. Semantic contours from inverse detectors. In *Intl. Conf. on Computer Vision*, 2011. 6, 8

[10] B. Hariharan, P. Arbelaez, R. Girshick, and J. Malik. Simultaneous detection and segmentation. In *ECCV*, 2014. 1, 6, 8

[11] K. He, X. Zhang, S. Ren, and J. Sun. Deep residual learning for image recognition. In *CVPR*, 2016. 6

[12] J. Hosang, R. Benenson, P. Dollár, and B. Schiele. What makes for effective detection proposals? *IEEE PAMI*, 17 Feb. 2015. 6

[13] H. Hu, S. Lan, Y. Jiang, Z. Cao, and F. Sha. FastMask: Segment multi-scale object candidates in one shot. 28 Dec. 2016. 1, 2, 6

[14] A. Kirillov, E. Levinkov, B. Andres, B. Savchynskyy, and C. Rother. InstanceCut: from edges to instances with Multi-Cut. 24 Nov. 2016. 3

[15] Y. Li, H. Qi, J. Dai, X. Ji, and Y. Wei. Fully convolutional instance-aware semantic segmentation. *arXiv preprint arXiv:1611.07709*, 2016. 2, 6, 8

[16] X. Liang, Y. Wei, X. Shen, Z. Jie, J. Feng, L. Lin, and S. Yan. Reversible recursive instance-level object segmentation. In *CVPR*, 2016. 1, 2, 6, 8

[17] X. Liang, Y. Wei, X. Shen, J. Yang, L. Lin, and S. Yan. Proposal-free network for instance-level object segmentation. *arXiv preprint arXiv:1509.02636*, 2015. 1, 2, 6, 8

[18] T.-Y. Lin, P. Dollár, R. Girshick, K. He, B. Hariharan, and S. Belongie. Feature pyramid networks for object detection. In *CVPR*, 2017. 2, 6

[19] A. Newell and J. Deng. Associative Embedding:End-to-End learning for joint detection and grouping. 16 Nov. 2016. 3, 8

[20] P. O. Pinheiro, R. Collobert, and P. Dollar. Learning to segment object candidates. In *NIPS*, 2015. 1, 2

[21] P. O. Pinheiro, T.-Y. Lin, R. Collobert, and P. Dollàr. Learning to refine object segments. In *ECCV*, 2016. 1, 2

[22] M. Ren and R. S. Zemel. End-to-End instance segmentation with recurrent attention. In *CVPR*, 2017. 3

[23] S. Ren, K. He, R. Girshick, and J. Sun. Faster R-CNN: Towards Real-Time object detection with region proposal networks. *IEEE Trans. Pattern Anal. Mach. Intell.*, 6 June 2016. 1, 2

[24] B. Romera-Paredes and P. H. S. Torr. Recurrent instance segmentation. In *ECCV*, 2016. 3

[25] F. Schroff, D. Kalenichenko, and J. Philbin. FaceNet: A unified embedding for face recognition and clustering. In *CVPR*, 2015. 1

[26] J. Shi and J. Malik. Normalized cuts and image segmentation. *IEEE PAMI*, 22(8):888–905, Aug. 2000. 1

[27] K. Sohn. Improved deep metric learning with multi-class n-pair loss objective. In *NIPS*, 2016. 4

[28] J. Uhrig, M. Cordts, U. Franke, and T. Brox. Pixel-level encoding and depth layering for instance-level semantic labeling. In *GCPR*, 2016. 3